CHAPTER 5

Amino acid composition, petrology, geochemistry, ^{14}C terrestrial age and oxygen isotopes of the Shisr 033 CR chondrite

We have analysed the Oman desert CR Shisr 033 using several different analytical techniques designed to study the degree of terrestrial alteration of this meteorite and also its petrologic classification. Bulk chemical analyses (including organic carbon and mean total H_2O content) show that a CR classification is accurate. Additionally, oxygen isotope analysis on a bulk sample indicates that Shisr 033 is of type CR2. Amino acid analysis using liquid chromatography with UV fluorescence detection (HPLC-FD) and liquid chromatography-time of flight-mass spectrometry (LC-ToF-MS) show that the absolute and the relative amino acid content of Shisr 033 is distinct from other carbonaceous chondrites, namely the CR Renazzo. Oxygen isotope analysis of a phyllosilicate-rich dark inclusion shows that this inclusion is closer to CV3 or CO3 chondrites. The effects of terrestrial weathering in Shisr 033 are evident by the dark inclusion carbon isotopic data, bulk chemistry (through the elevated concentrations of Sr and Ba), and amino acid data suggesting extensive amino acid contamination of the meteorite from the fall site soil. Nevertheless, Shisr 033 contains a small fraction of indigenous components, as indicated by the presence of the extraterrestrial amino acid α-aminoisobutyric acid (α-AIB) that was not detected in the Shisr soils. Finally, the terrestrial age of Shisr 033 was determined and discussed in the context of high levels of contamination.

Z. Martins, B. A. Hofmann, E. Gnos, R. C. Greenwood, A. Verchovsky, I. A. Franchi, A. J. T. Jull, O. Botta, D. P. Glavin, J. P. Dworkin, P. Ehrenfreund (2006)
Meteoritics & Planetary Science, submitted.

5.1 Introduction

Hot deserts (including Australia, western USA, North Africa and the Arabian Peninsula) became a source of an increasing number of meteorite finds in the past years (Jull *et al.* 1990; Ash and Pillinger 1995 and references given; Bischoff and Geiger 1995; Al-Kathiri *et al.* 2005). The meteorites collected in these arid areas suffer physical and chemical alterations known as weathering. These terrestrial alteration effects were studied previously by other authors, and different techniques were used to quantify the weathering degree. For example, ^{57}Fe Mössbauer spectroscopy (Bland *et al.* 1996a, 1998a, 1998b; Franchi *et al.* 1996) is a well known technique used to determine the degree of oxidation in the meteorites. Additionally, changes in the isotopic composition (Bland *et al.* 1996b) and in the chemical composition were determined, using, among other techniques, atomic emission spectrometry (ICP-AES) (Stelzner et al. 1999; Gillet et al. 2005), stepped-combustion analysis (Ash and Pillinger 1995), evolved gas analysis (Stelzner and Heide 1996; Stelzner *et al.* 1999), X-Ray fluorescence spectroscopy (XRF) (Bland *et al.* 1998b), electron probe analysis (EPMA) (Lee and Bland 2004), backscattered electron spectrometry (BSE) and mass spectrometry (ICP-MS) (Gillet *et al.* 2005).

In this study we performed an interdisciplinary analysis of the Shisr 033 meteorite. Shisr 033 is the first CR carbonaceous chondrite to be recovered from the Oman desert (in October 2002), and it consists of 65 fragments with a total mass of 1098g recovered from an area of a few square meters. A unique feature of Shisr 033 is the presence of millimeter-sized dark inclusions that were thought to be similar to CI-type carbonaceous chondrites (Russell *et al.* 2004). The goals of this study were to investigate how terrestrial alteration has changed the organic, chemical, mineralogical and isotopic composition of the meteorite as well as the dark-CI-like inclusions. Hence, major and trace elements, iron and volatiles abundances were obtained for the Shisr 033 meteorite. In addition, amino acid abundances of Shisr 033 were measured and compared to (1) CM- and CI-type carbonaceous chondrites, (2) two ordinary chondrites collected in the same area, and (3) desert soil samples collected on the proximities of the meteorite fall site location. We have also investigated the oxygen and carbon isotopes of Shisr 033 and compared these values to other meteorite classes. Finally, we have also determined the terrestrial ages of Shisr 033 and of the other chondrites collected in the Oman desert.

5.2 Materials and Methods

5.2.1 Samples and sample preparation

Shisr 033 (a CR chondrite), Shisr 031 and Shisr 035 (both L6 chondrites), and three soil samples (named 78, 82 and 89) were collected in Oman (Fig. 5.1) by a joint meteorite search program (Al-Kathiri *et al.* 2005). A large Shisr 033 meteorite fragment (249.9 g) was selected for analysis and interior material was obtained by splitting away the surface. The interior fragment was then crushed and homogenised into powder, from which a fines fraction (4.86 g) enriched in phyllosilicate-rich material was selected for the amino acids and oxygen isotopes analysis. Individual phyllosilicate-rich dark inclusions were selected for oxygen and carbon isotope analysis, as well as individual chondrules picked from the coarse material for the oxygen isotope analysis. A large piece of Murchison meteorite (6.294 g, USNM 6650) was provided by the Smithsonian National Museum of Natural History, Washington DC. Orgueil meteorite (7.76 g) was provided by the Musée National d'Histoire Naturelle, Paris. The Murchison, Orgueil, Shisr 031 and Shisr 035 meteorites, together with the three soil samples (78, 82 and 89) were separately ground and homogenised into powder using a ceramic mortar and pestle in a glovebox containing argon and were stored in sterilised glass vials before being analysed. A serpentine (hydrated magnesium silicate) sample, provided by the Natural History Museum, Bern, was crushed into powder in the same glove box, heated to 500°C for 3 h prior to analysis, subjected to the same processing procedure as the meteorites and soil samples and used as a procedural blank.

Powdered aliquots of Tiffa 001 (a H5 with weathering degree W2), and Grein 003 (a H6 with a lightly weathering degree W1), collected in the Tenere region of Niger, were used in our study (for the oxygen isotope analysis) to test the efficiency of the ethanolamine-thioglycollate washing method in removing terrestrial weathering products and its effects on the indigenous oxygen isotopic composition of the meteorite samples.

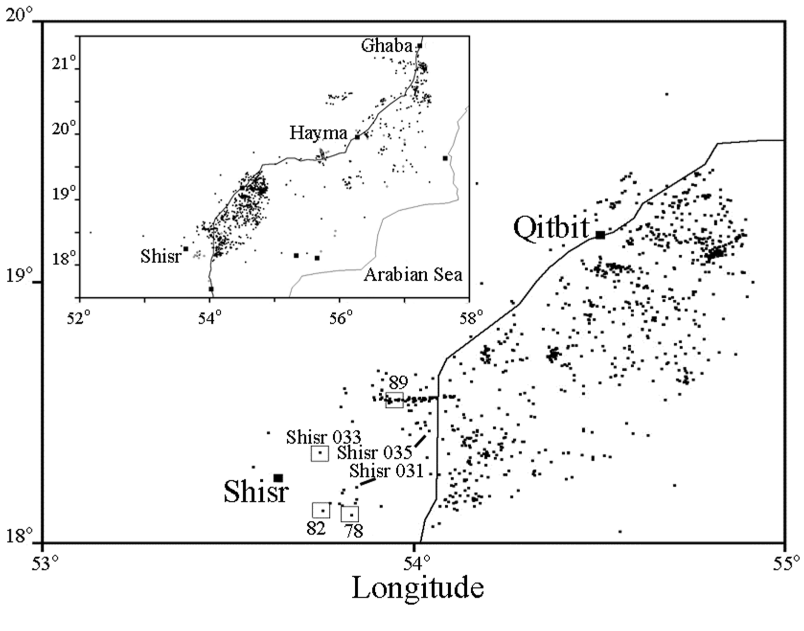

Fig. 5.1 - Map showing the fall site of Shisr 031, Shisr 033, and Shisr 035 meteorites and the places where the soil samples were collected, here named 78, 82 and 89. The inset shows the map of part of the Sultanate of Oman, bordered by the Arabian Sea. One degree is about 111 Km.

5.2.2 Chemicals, reagents and tools

Amino acid standards (except D- and L-isovaline), sodium acetate trihydrate, sodium borate decahydrate, HPLC-grade water, *o*-phthaldialdehyde (OPA) and N-acetyl-L-cysteine (NAC) were purchased from Sigma-Aldrich. Ammonium hydroxide (28-30 wt%), D- and L-isovaline standards were purchased from Acros Organics. Methanol (absolute HPLC) was acquired from Biosolve Ltd, sodium hydroxide and hydrochloric acid (37%) from Boom, and AG® 50W-X8 cation exchange resin (100-200 mesh) from Bio-Rad. All the tools, glassware and ceramics used in the amino acid analysis were sterilized by annealing in aluminium foil at 500°C for 3 h. In addition, all tips and Eppendorf tubes used in the same analysis were supplied sterilized from Sigma-Aldrich.

5.2.3 Petrology and chemistry analysis

The petrology of Shisr 033 was investigated using a polished thin section of 5.9 cm^2 surface with transmitted and reflected light microscopy. Mineral compositions were determined using a Cameca SX-50 microprobe equipped with wavelength-dispersive spectrometers using natural and synthetic mineral standards and beam conditions of 15 kV and 20 nA. Data were corrected using the PAP procedure (Pouchou and Pichoir 1984). Cathodoluminescence (CL) images were obtained using a high-sensitivity CL-microscope (Ramseyer *et al.* 1989) equipped with a computer-controlled digital camera system (ColorView 12 run under analySIS FIVE image analysis program). Beam conditions applied were 0.2-0.4 $\mu A/mm^2$ and 25 keV. Iron hydroxides were removed from certain sample fractions for oxygen isotope (see section 5.2.5.) and iron analyses using ethanolamine thioglycollate (Cornish and Doyle 1984) in solution with an equal volume of isopropanol. Samples were leached until the production of the red iron complex ceased, indicating that all iron hydroxides were dissolved, and then washed in deionised water. This treatment removes iron oxides, hydroxides and metallic iron, but not silicate-bound iron.

The bulk chemistry was obtained by lithium metaborate/tetraborate fusion and combined inductively coupled plasma-mass spectrometry (ICP-MS) and inductively coupled plasma-optical emission spectroscopy (ICP-OES; analysis code 4 lithoresearch). Bulk iron was determined at the Activation Laboratories using ICP-OES, and the total carbon and CO_2 were determined by combustion/infrared detection using oxygen and an inert gas, respectively. The organic carbon is obtained by difference.

5.2.4 Amino acid extraction procedure, HPLC-FD and LC-ToF-MS analysis

Approximately 100 mg each of Shisr 033, Shisr 031, Shisr 035, Murchison, and Orgueil meteorites, together with Shisr landing site soil samples (named 78, 82, and 89) and a serpentine control blank were analysed using the established procedure for extracting, separating and analysing amino acids in meteorites (Zhao and Bada 1995; Botta *et al.* 2002; Glavin *et al.* 2006). Each of these powdered samples was flame sealed inside a test tube (20 x 150 mm) together with 1 ml of HPLC water and heated for 24 h in a heating block (temperature set at 100°C). After the hot water extraction, the test tubes were rinsed with HPLC water, cracked open, and centrifuged. One of two equal parts of the water supernatants was then transferred to a smaller tube (10 x 75 mm), dried under vacuum, flame sealed inside a test tube (20 x 150 mm) containing 1 ml of 6 M HCl, and subjected to acid vapour hydrolysis for 3 h, at 150°C. The test tubes were then rinsed with HPLC water and cracked open; the small tubes were removed and dried under vacuum. The hydrolysed extracts were brought up in 3 ml of HPLC water, desalted on a cation exchange resin, and the amino acids eluted from the resin with 5 ml of 2 M ammonium hydroxide. These eluates were dried under vacuum, and derivatised (Zhao and Bada 1995) with *o*-phthaldialdehyde/N-acetyl-L-cysteine (OPA/NAC) separately at the Leiden Institute of Chemistry and then at NASA Goddard. At the Leiden Institute of Chemistry, the dried ammonium hydroxide eluates were brought up in 100 µl HPLC water, and 10 µl aliquots were added to 10 µl of 0.1 M sodium borate buffer in Eppendorf vials. These were dried under vacuum to remove any residual ammonia, brought up in 20 µl of sodium borate buffer, and then derivatised with 5 µl of OPA/NAC. The derivatisation was quenched after 1 or 15 min by adding 475 µl of 50 mM sodium acetate buffer (mobile phase). At NASA Goddard, the same extracts were derivatised using the same procedure and then quenched after 1 or 15 minutes with 75 µl of 0.1 M hydrazine hydrate. OPA/NAC amino acid derivatives were analysed by HPLC-FD at the Leiden Institute of Chemistry, and by simultaneous HPLC-FD and ToF-MS at NASA Goddard. HPLC-FD analysis at Leiden was carried out in a C18 reverse phase (250 x 4.6 mm) Synergi 4µ Hydro-RP 80A column (from Phenomenex), flow rate 1 ml min^{-1}, and UV fluorescence detection on a Shimadzu RF-$10A_{XL}$ (excitation wavelength at 340 nm and emission at 450 nm). The conditions for amino acid separations for the mobile phase at 25°C were as follows: Buffer A was 50 mM sodium acetate, containing 4% methanol (v/v), and buffer B was methanol. The gradient used was 0 to 4 min, 0% buffer B; 4 to 5 min, 0 to 20% buffer B; 5 to 10 min, 20% buffer B; 10 to 17 min, 20 to 30% buffer B; 17 to 27 min, 30 to 50% buffer B; 27 to 37 min, 60% buffer B; 37 to 49 min, 60% buffer B; 49 to 50 min, 60 to 0% buffer B; 50 to 60 min, 0% buffer B. Amino acids were identified by retention time comparison with known standards. LC-ToF-MS analyses at NASA Goddard were carried out according to the procedures described by Glavin *et al.* (2006). In all analyses the amino acid abundances (part per billion by weight) in the samples were calculated by comparing the integrated peak area, corrected for the abundances in the serpentine blank sample, with the integrated peak area of known amino acid standards.

5.2.5 Oxygen and carbon isotope analysis

Oxygen isotope analyses were performed on 4 samples of the Shisr 033 meteorite: a whole rock sample (WR), a whole rock sample washed in ethanolamine thioglycollate (washed WR), a composite of hand picked chondrules and a hand picked phyllosilicate-rich inclusion (D). In addition powdered aliquots of the Tiffa 001 meteorite, and the Grein 003 meteorite were washed in ethanolamine thioglycollate (see section 5.2.3. for more details) until the solution barely changed colour, rinsed in water, finally in isopropanol and dried before analysis.

Oxygen isotopes were performed by laser fluorination. Samples of 1 to 2 mg of powdered material are heated with a CO_2 laser (10.6 μm) in the presence of approximately 200 torr of BrF_5. The oxygen gas liberated is purified cryogenically and chemically before analysis on a PRISM III (VG Micromass, UK) dual inlet mass spectrometer. Analytical precision is ±0.08‰ for $\delta^{18}O$ and ±0.04‰ for $\delta^{17}O$. Details of the method are given by Miller *et al.* (1999).

Carbon isotope measurements were performed on the phyllosilicate-rich dark inclusion (D). A sample of 0.423 mg of crushed material was step combusted in 50˚C and 100˚C increments, the gas at each heating step purified and the abundance and isotopic composition of carbon (as CO_2) measured. The mass spectrometer used is a modified SIRA 24 (VG Micromass, UK) re-designed to operate in static vacuum mode. The system is readily capable of analysing less than 1 nmole of carbon with a precision for $\delta^{13}C$ of approximately ±1‰. Details of the analytical technique are given by Wright and Pillinger (1989).

5.2.6 Terrestrial age analysis

The terrestrial ages of the Shisr 033, Shisr 031 and Shisr 035 meteorites (See Table 5.10 for the samples mass) were determined by accelerator mass spectrometry (AMS) of cosmic ray-produced ^{14}C. Untreated and acid-etched (used to remove any weathering products) samples, as well as a sample of Shisr 033 treated both by acid etching and with ethanolamine thioglycollate (used to remove iron hydroxides as referred before) were measured. Additional sample treatment included preheating to 500°C in air to remove terrestrial organic contaminants, followed by fusion of the sample with iron using RF furnace heating in oxygen to produce CO_2. Further sample preparation, ^{14}C extraction and AMS measurement procedures are described elsewhere (Jull *et al.* 1989; 1990; 1993; 1998).

5.3. Results and Discussion

5.3.1 Petrology

Shisr 033 was classified as a CR chondrite (Russell *et al.* 2004) based on the reduced character of silicates (olivine with $Fa_{2-7.9}$ by electron microprobe; Fe-poor pyroxene, $Fs_{1.2-12.1}$) and the presence of phyllosilicate-rich inclusions.

Representative olivine and pyroxene analyses performed in this study are listed in Table 5.1. A low metamorphic grade (3 or lower) is supported by cathodoluminescence images (Fig. 5.2) showing a very heterogeneous and unequilibrated texture. This is spectacularly expressed by bright yellow and red, greenish and blue colors of chondrule minerals and glass under the cathode. Many chondrules show abrupt or gradual color zoning. The luminescence activity of enstatite and forsterite is caused by traces of Cr and Mn (e.g., Steele *et al.* 1990). At higher metamorphic grade the cathode luminescence colors are suppressed by the higher iron-contents in forsterite and enstatite. The average chondrule

Table 5.1 - Representative microprobe analyses of the Shisr 033 silicates.

Mineral	**Olivine**			**Pyroxene**		
SiO_2 (wt%)	42.27	42.13	41.55	56.35	56.42	57.63
TiO_2	b.d.	b.d.	b.d.	0.16	0.11	0.10
Al_2O_3	0.02	0.11	0.01	2.94	0.94	0.82
Cr_2O_3	0.59	0.89	0.74	0.76	0.89	0.81
FeO	2.60	2.41	6.82	4.09	4.58	3.45
MnO	0.26	0.24	0.99	0.48	0.47	0.14
NiO	0.04	0.05	b.d.	0.04	0.22	0.20
MgO	54.70	54.90	50.60	33.51	35.64	37.04
CaO	0.19	0.21	0.26	1.68	0.62	0.55
Na_2O	b.d.	b.d.	b.d.	0.16	b.d	0.04
K_2O	b.d.	b.d.	b.d.	b.d.	b.d	b.d
Total	100.68	100.94	101.15	100.19	100.12	100.98
Si (a.f.u.†)	0.999	0.993	1.000	1.935	1.937	1.948
Ti	-	-	-	0.004	0.003	0.002
Al	0.001	0.003	0.004	0.119	0.039	0.039
Cr	0.011	0.017	0.014	0.021	0.024	0.022
Fe	0.051	0.047	0.138	0.118	0.132	0.098
Mn	0.005	0.005	0.020	0.014	0.014	0.018
Ni	0.001	0.001	-	0.001	0.006	0.006
Mg	1.927	1.928	1.816	1.715	1.824	1.791
Ca	0.005	0.005	0.007	0.062	0.023	0.020
Na	-	-	-	0.011	-	0.002
K	-	-	-	-	-	-
Fa/Fs	0.026	0.024	0.069	0.062	0.038	0.025
Wo/Or				0.034	0.012	0.010

b.d. - below detection
a.f.u. - atoms per formula unit

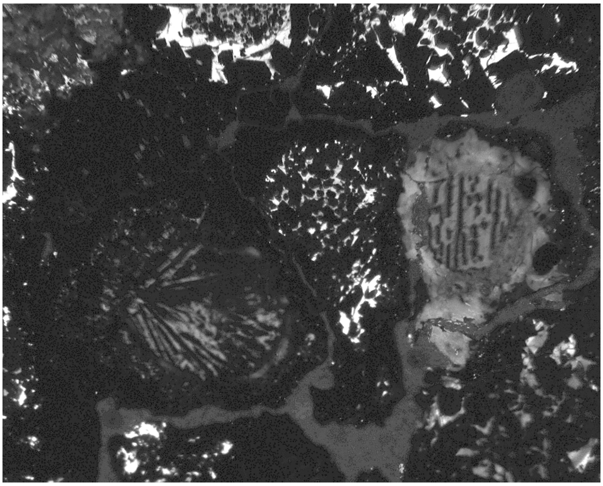

Fig. 5.2 - Cathodoluminescence (CL) image of a polished thin section of Shisr 033 showing the unequilibrated nature expressed by coexisting yellow, red, greenish and blue CL colours of chondrule minerals and glass. Field of view is 3.8 mm. Colour picture available on the back flap of the thesis cover.

size of PO, POP, PP, BO and RP chondrules is 1.0 mm and the matrix/chondrule + aggregate ratio is 0.53. Large metal grains and metal-rich PO chondrules are common.

Shisr 033 contains <10 vol% dark, soft inclusions up to 5 mm in size, originally classified as CI (Russell *et al.* 2004). These inclusions show the presence of smectitic (possible smectite-chlorite mixed-layer clay minerals) phyllosilicates in XRD-patterns (peak at ~15Å). In polished thin sections laths of pyrrhotite and fine-grained (framboidal) magnetite are recognized in a fine-grained matrix. These inclusions clearly correspond to the dark inclusions in CRs described by Weisberg *et al.* (1993) both in terms of mineralogy and mode of occurrence.

The meteorite shows minor weathering of the metal (W2), but this is based only on limited alteration of metallic iron. Still, iron hydroxides released during weathering impregnate the meteorite, including the dark inclusions, giving the meteorite a generally yellow-brown rusty appearance.

5.3.2 Chemistry

Bulk chemistry data were obtained on two bulk samples (from which some large metal nuggets were excluded due to grinding problems) and on the fraction of fines used for amino acid analysis (Table 5.2). Data for volatiles (C, CO_2 and H_2O) are presented in Table 5.3. Data obtained on Shisr 033 are compared with CR analyses discussed in Bischoff *et al.* (1993). Shisr 033 has a very similar bulk composition as the averaged CR chondrites (Table 5.2). The slightly lower iron content might be due to the exclusion of some large metal nuggets. Compared with bulk analyses, the fines fraction of Shisr 033 used for amino acid analysis is slightly enriched in iron and volatiles, including organic carbon, and slightly depleted in Mg, but is close in composition to the bulk meteorite. Iron enrichment is probably due to a higher iron content of dark inclusions combined with iron hydroxide accumulation from altered iron metal preferentially enriched in the fine-grained fraction. As evidenced from total iron data of ethanolamine thioglycollate leached samples (Table 5.3) about 70% of iron is easily leached and thus present in oxide- or metallic form. The silicate fraction contains 6.1 to 6.7 wt% iron, consistent with mineral analyses by electron microprobe (Table 5.1). Rare Earth Elements (REE) are present at typical chondritic concentrations (Anders and Grevesse 1989) with no significant evidence of fractionation. Repeat analyses on different subsamples indicate an organic carbon content in the bulk meteorite of 0.29% ± 0.03%, lower than in Renazzo, Al Rais, EET 87770 and Y-790112, but similar to CR's from the Sahara (Bischoff *et al.* 1993). Assuming that most of the organic carbon is concentrated in fine-grained dark inclusions that represent <10% of the rock, a concentration of several wt% carbon is required in these inclusions. The mean total H_2O content of Shisr 033 is 6.07% (Table 5.3), similar to Renazzo (5.67 wt%) and Al Rais (8.49 wt%) (Weisberg *et al.* 1993). Bulk chemical analyses are, therefore, consistent with the CR classification of Shisr 033 (see section 5.3.1.). An unknown fraction of H_2O in the fines (Table 5.3) is likely due to terrestrial weathering (mainly in iron-hydroxides). Furthermore, the effects of terrestrial weathering are seen in the elevated concentrations of Sr and Ba (Table 5.2).

5.3.3 Amino Acid composition and terrestrial contamination

We have analysed the amino acid composition of the desert meteorite CR Shisr 033. Fig. 5.3 shows a typical HPLC-FD chromatogram of the acid hydrolysed hot-water extracts of the Shisr 033, Orgueil and Murchison meteorites, and a serpentine blank, measured at the Leiden Institute of Chemistry. The corresponding amino acid abundances are displayed in Table 5.4. The most abundant amino acids present in the Shisr 033 meteorite extract include L-alanine (738 ppb), L-glutamic acid (687 ppb), glycine (548 ppb) and L-aspartic acid (315 ppb). The abundances of amino acids in the Shisr 033 meteorite were independently verified by LC-ToF-MS at NASA Goddard. Fig. 5.4 displays a typical HPLC-FD chromatogram of the Shisr 033, Shisr 031, and Shisr 035 meteorites, soil sample 78, and a serpentine blank, and Fig. 5.5 displays both HPLC-FD and ToF-MS chromatograms of the Shisr 033 meteorite acid hydrolysed hot-water extract measured at NASA Goddard. All the corresponding amino acid abundances are shown in Table 5.5. In accordance with the HPLC-FD data, the most abundant amino acids in Shisr 033 determined by LC-ToF-MS are L-glutamic acid (489 ppb), glycine (417 ppb), L-alanine (330 ppb), and L-aspartic acid (189 ppb). A comparison of the Shisr 033 amino acid content determined by HPLC-FD (Table 5.4) and by LC-ToF-MS (Table 5.5) shows that the abundances generally agree within the experiment uncertainties. However, for L-glutamic acid, β-alanine and L-alanine the abundances measured by LC-ToF-MS are lower than by HPLC-FD. The difference may be explained due to the fact that the amino acid identification by HPLC-FD is based only on retention

Table 5.2 - Chemical composition of the CR type carbonaceous chondrite Shisr 033 (in two bulk samples and in fines) as measured by ICP-MS/ICP-OES. For comparison, literature CR type carbonaceous chondrites bulk data are shown.

	Shisr 033			Renazzo[b]	Al Rais[b]	Average CR[c]
Elements	**Bulk**	**Bulk**	**Fines[a]**			
Si (wt%)	15.79	15.67	15.53	15.81	14.14	
Ti	0.06	0.06	0.06	0.11	0.05	
Al	1.21	1.17	1.08	1.25	1.04	1.18
Fe	21.47	21.66	23.67	24.93	23.78	23.58
Mn	0.16	0.16	0.16	0.18	0.18	0.17
Mg	13.86	13.82	12.10	14.33	12.78	13.21
Ca	1.55	1.51	1.50	1.27	1.43	1.29
Na	0.15	0.15	0.18	0.41	0.46	0.33
K	<0.008	0.02	<0.008	0.03	0.03	0.03
P	0.08	0.08	0.09	0.12	0.12	
LOI[†]	6.46	6.22	7.61	7.17	11.17	
V (ppm)	81	71	70	78	70	72
Cr	3970	3430	3410	3740	3250	3558
Co	627	548	629	680	616	650
Ni	>10,000	>10,000	>10,000	13600	12600	13591
Cu	96	78	108			80
Zn	79	66	88	94	162	106
Ga	4.85	4.37	5.55	5.2	6.80	5.4
Ge	9.26	7.61	10.84			
As	<5	<5	<5	2.93	1.47	1.6
Rb	1.46	1.59	1.76			
Sr	148	129	162			
Y	2.69	2.25	2.23			
Zr	11.33	7.73	7.28			
Nb	0.75	0.59	0.59			
Mo	<2	<2	<2			
Ag	<0.5	<0.5	<0.5			
In	<0.1	<0.1	<0.1			
Sn	1.87	1.31	1.63			
Sb	<0.2	<0.2	<0.2	0.072	0.098	0.08
Cs	<0.1	0.11	0.11			
Ba	9.74	6.57	11.25			
La	0.43	0.38		0.319	0.3	0.31
Ce	1.18	1.04				0.89
Pr			0.19			
Nd			0.81			0.5
Sm	0.24	0.25	0.20	0.2	0.186	0.212
Eu	0.09	0.08	0.09	0.079	0.074	0.081
Gd	0.36	0.37	0.26			
Tb	0.11	0.10	0.05			0.05
Dy	0.68	0.66	0.34			0.32
Ho	0.08	0.08	0.07			0.1
Er	0.24	0.22	0.21			
Tm	0.04	0.04	0.04			

Table 5.2 *Continued* - Chemical composition of the CR type carbonaceous chondrite Shisr 033 (in two bulk samples and in fines) as measured by ICP-MS/ICP-OES. For comparison, literature CR type carbonaceous chondrites bulk data are shown. All values are reported in wt%.

	Shisr 033					
Elements	**Bulk**	**Bulk**	**Fines[a]**	**Renazzo[b]**	**Al Rais[b]**	**Average CR[c]**
Yb (ppm)	0.23	0.23	0.23	0.223	0.211	0.227
Lu	0.03	0.03	0.03	0.033	0.03	0.033
Hf	0.20	0.19	0.16			0.18
Ta	0.04	0.02	0.03			0.045
Tl	<0.05	0.06	<0.05			
Pb	<5	<5	<5			
Bi	<0.1	<0.1	<0.1			
Th	0.11	0.08	0.25			
U	0.04	0.04	0.08			

[†]Loss on ignition.
[a]Same fraction as used for amino acid analysis.
[b]Weisberg et al. (1993); Kallemeyn and Wasson (1982).
[c]From Bischoff et al. (1993).

Table 5.3 - Percentage (%) of iron and volatiles in different sub-samples of the CR type carbonaceous chondrite Shisr 033 (bulk samples and fines) as measured, respectively, by ICP-OES, and by combustion/infrared detection.

Sample	**C total**	**CO_2**	**C organic**	**$H2O^-$**	**$H2O^+$**	**Fe total**
Bulk	0.31	0.20	0.25	1.53	4.56	21.47
Bulk	0.31	<0.01	0.30	1.60	4.46	21.66
Bulk	0.32	<0.01	0.32	1.29	4.88	21.02
Bulk	0.30	<0.01	0.30	1.40	4.52	21.72
Mean bulk	**0.31**	**<0.01**	**0.29**	**1.46**	**4.61**	**21.47**
Bulk ETG-leached*						6.69
Bulk ETG-leached*						6.09
Fines**	0.34	<0.01	0.34	n.a.	n.a.	23.67

*Ethanolamine thioglycollate leach, it removes iron hydroxides.
**Fraction used for amino acid analysis
n.a. - not analysed

time comparison, while the identification by LC-ToF-MS is in addition based on the exact molecular mass of the eluting compounds. Therefore, it cannot be excluded that there could be a small fraction of co-eluting compounds contributing to the fluorescence signal intensity in HPLC-FD analyses. In any case, this will not change the overall amino acid distribution in the Shisr 033 meteorite. Amino acid distribution provides important clues about the degree of terrestrial contamination and therefore to the weathering degree suffered by the meteorite. There are three ways to evaluate the source of amino acids present in carbonaceous chondrites (see Botta and Bada 2002): (1) determination of the D/L enantiomeric ratios for chiral amino acids, with a racemic ratio (D/L ~ 1) indicating an abiotic synthetic origin, (2) the presence of extraterrestrial amino acids, including α-aminoisobutyric acid (α-AIB) and isovaline in the meteorite extract, and (3) measurement of compound-specific stable isotope ratios of hydrogen, carbon, and/or nitrogen. In the present study, the abundance of amino acids extracted from the available 100 mg sample of Shisr 033 is below the detection limit of current state of the art gas chromatography isotope ratio mass spectrometers, preventing the use of this method. With regard to (1), our amino acid data show that L-amino acids are significantly more abundant than D-amino acids in Shisr 033 (Table 5.4 and 5.5), clearly indicating the presence of terrestrial contamination in these samples. Additionally, we calculated the amino acid enantiomeric ratios (Table 5.6) in the Shisr 033 for four protein amino acids (aspartic acid, glutamic acid, alanine and valine). The D/L ratio values obtained by HPLC-FD and LC-ToF-MS, agree with each other within the experimental error. All values were found to be smaller than 0.4, which is an indication of a high terrestrial contamination level. The only exception is the D/L alanine ratio of 0.83 ± 0.15, obtained by LC-ToF-MS, and therefore we cannot exclude the presence of extraterrestrial components in this meteorite. The D/L alanine ratios in the soil samples (Tables 5.5 and 5.6) range from 0.29 to 0.45, with D-alanine probably coming from the racemisation of microbial detritus in the soil. If the alanine present in the Shisr 033 meteorite was all due to contamination then its D/L ratio would be expected to fall within the same range. Clearly, the D/L alanine ratio of 0.83 ± 0.15 in Shisr 033 is significantly higher, and can best be explained by an initial D/L alanine ratio in the Shisr 033 meteorite of ~1 and a subsequent L-alanine contamination of the meteorite after its fall to Earth leading to the lower ratio observed today in the meteorite. Finally, with regard to (2), a small quantity of α-AIB was detected in Shisr 033 both by HPLC-FD (34 ± 5 ppb; Table 5.4) and LC-ToF-MS (38 ± 3ppb; Table 5.5). However, no isovaline or β-amino-*n*-butyric acid were detected (both at the same level as the detection limit; Table 5.4 and 5.5). As a terrestrial contamination control we also analysed the amino acid content of two L6 chondrites (Shisr 031 and Shisr 035) collected in the same area as the Shisr 033 meteorite (Fig. 5.1). Those meteorites are not expected to contain any indigenous amino acid, as they were heated to >800ºC in the parent body (Slater-Reynolds and McSween 2005 and references given in there), and therefore all amino acids observed will be due to terrestrial contamination from the meteorite fall site. Table 5.5 shows the amino acid abundances in the acid hydrolysed hot-water extracts of Shisr 031 and Shisr 035 meteorites, measured by LC-ToF-MS. In the case of Shisr 031, glycine and glutamic acid are the most abundant amino acids with concentrations of 24 and 6 ppb, respectively. All other amino acids are present at even lower abundance or are below the limit of detection. In the case of the Shisr 035 meteorite, the degree of terrestrial contamination is higher than for Shisr 031, containing aspartic acid (398 ppb for the L- and 126 ppb for the D-enantiomer), glutamic acid (156 ppb for the L- and 50 ppb for the D-enantiomer), alanine (49 ppb for the L- and 28 ppb for the D-enantiomer) and glycine (41 ppb) as the most abundant amino acids. All these amino acids are typical components of bacteria (e.g. Howe *et al.* 1965). Comparison of the amino acid content of the L6 chondrites to the amino acid content of the CR Shisr 033 can be used to determine which amino acids may be in part (or totally) due to terrestrial contamination.

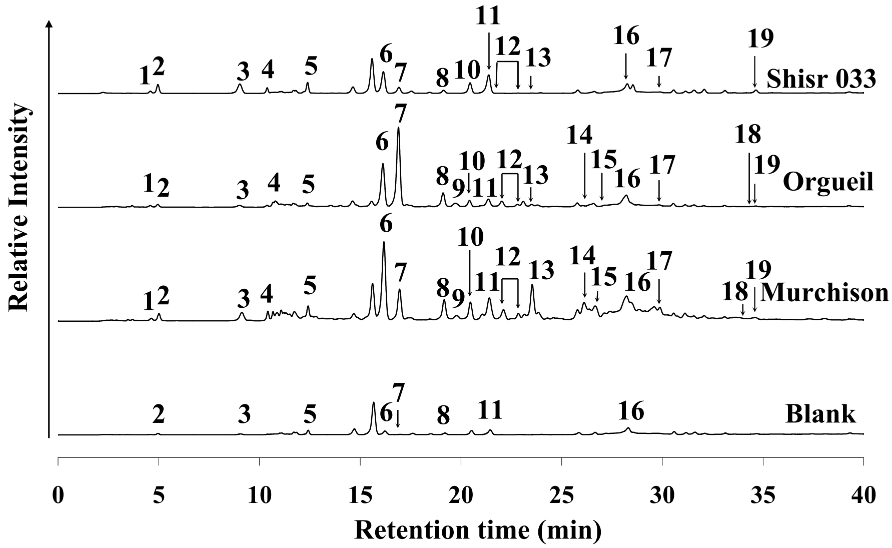

Fig. 5.3 - The 0 to 40 min region (no peaks were observed outside this region) of the HPLC-FD chromatograms. OPA/NAC derivatisation of amino acids in the 6M HCl-hydrolysed hot-water extracts from the CM2 carbonaceous chondrite Murchison, the CI1 Orgueil, the CR Shisr 033, and the serpentine blank. The peaks were identified by comparison of the retention time to those in the amino acid standard run on the same day: 1. D-aspartic acid; 2. L-aspartic acid; 3. L-glutamic acid; 4. D-glutamic acid; 5. D, L-serine; 6. glycine; 7. β-alanine; 8. γ-amino-*n*-butyric acid (γ-ABA); 9. D,L-β-aminoisobutyric acid (D, L-β-AIB); 10. D-alanine; 11. L-alanine; 12. D, L-β-amino-*n*-butyric acid (D, L-β-ABA); 13. α-aminoisobutyric acid (α-AIB); 14. D-isovaline; 15. L-isovaline; 16. L-valine; 17. D-valine; 18. D-leucine; 19. L-leucine.

Since glutamic acid and glycine were detected in both ordinary chondrites, it can be concluded that at least a fraction of their abundances in Shisr 033 is due to terrestrial contamination. It is also interesting to note the very low content of ε-amino-*n*-caproic acid (EACA). This amino acid is a contaminant derived from nylon bags frequently used to store meteorite samples (Glavin *et al.* 2006). Since all the meteorites analysed in our study were collected in aluminium foil and polypropylene bags, it is not surprising that no EACA has been detected.

In an attempt to understand why the amino acid contamination is not uniform in the two ordinary chondrites studied, we have analysed Oman desert soils from three different locations (Fig. 5.1) by LC-ToF-MS. Fig. 5.4 displays a typical HPLC-FD chromatogram of the soil 78 acid hydrolysed hot-water extract and a serpentine blank, with the amino acid content of all three soil samples compiled in Table 5.5. In contrast to previous analysis that showed that the chemical composition of the Oman desert soil is uniform (Al-Kathiri *et al.* 2005), our data show that the amino acid distribution is not uniform in these three soils. The total amino acid abundances measured in these samples are 1040 ppb, 200 ppb, and 90 ppb for soils 78, 82 and 89, respectively. Despite these quantitative

Table 5.4 - Summary of the average total amino acid abundances (in ppb) in the 6 M HCl acid hydrolysed hot-water extracts of the CM2 carbonaceous chondrite Murchison, CI1 carbonaceous chondrite Orgueil and CR type carbonaceous chondrite Shisr 033 as measured by HPLC-FD[a].

Amino Acid	**CM2 Murchison**	**CI1 Orgueil**	**CR Shisr 033**
D-Aspartic Acid	98 ± 5	83 ± 9	86 ± 1
L-Aspartic Acid	182 ± 10	101 ± 22	315 ± 32
D-Glutamic Acid	292 ± 20	45 ± 8	164 ± 15
L-Glutamic Acid	479 ± 34	111 ± 19	687 ± 40
D,L-Serine[†]	271 ± 63	386 ± 100	266 ± 97
Glycine	1429 ± 66	1040 ± 191	548 ± 123
β-Ala	1007 ± 73	2784 ± 212	173 ± 7
γ-ABA	647 ± 76	410 ± 40	42 ± 3
D-Alanine	617 ± 21	220 ± 40	290 ± 11
L-Alanine	708 ± 96	286 ± 42	738 ± 53
DL-β-ABA[‡]	529 ± 11	399 ± 17	<10 ± 2*
DL-β-AIB[‡]	353 ± 19	218 ± 20	<2 ± 1*
α-AIB	1923 ± 275	73 ± 23	34 ± 5
D-Isovaline	2493 ± 513	52 ± 33	< 6 ± 2*
L-Isovaline	2297 ± 316	74 ± 27	< 6 ± 1*
D-Valine	395 ± 42	80 ± 4	20 ± 16
L-Valine	737 ± 205	346 ± 61	209 ± 49
D-Leucine	110 ± 30	17 ± 5	< 15 ± 5*
L-Leucine	104 ± 10	72 ± 31	199 ± 25
Total	**14700**	**6800**	**3800**

[a]Quantification of the amino acids included background level correction using a serpentine blank. The associated errors are based on the standard deviation of the average value between three and four separate measurements (N) with a standard error, $\delta x = \sigma_x \cdot N^{-1/2}$.
*These concentrations were very similar to blank levels and therefore were considered to be maximum values.
[†]Enantiomers could not be separated under the chromatographic conditions.
[‡]Optically pure standard not available for enantiomeric identification.

differences there is some qualitative agreement as in all soils the most abundant amino acids are the L-amino acids and glycine. Non-protein amino acids (including α-AIB) are absent in the soil, which indicates that there was no leaching of amino acids from any meteorite present in the surroundings into the soil. Comparison of the protein amino acid enantiomeric ratios (Table 5.6) of Shisr 033 to those of the soil shows agreement within the experimental error, and in all cases the ratios are smaller than 0.4, indicating that, with the exception of a small extraterrestrial component (see above), most of the amino acids in the Shisr 033 meteorite are terrestrial in origin. Possible reasons for the higher contamination in Shisr 033 than in the two ordinary chondrites will be discussed in section 5.3.5.

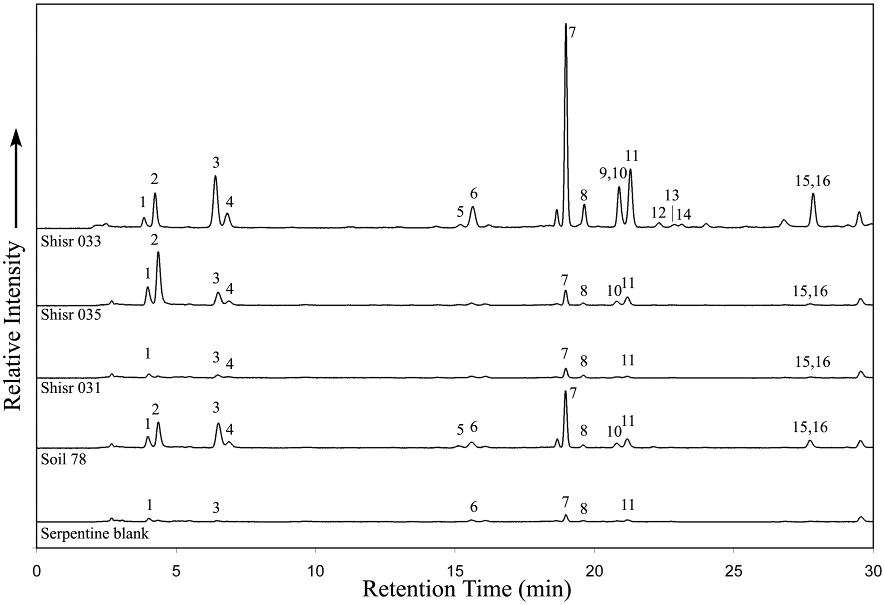

Fig. 5.4 - The 0 to 30 min region of the HPLC-FD chromatograms from the NASA Goddard analyses. OPA/NAC derivatisation of amino acids in the 6M HCl-hydrolysed hot-water extracts from the Shisr 033, Shisr 031, and Shisr 035 meteorites, soil sample (78), and serpentine blank. The peaks were identified by comparison of the retention time and exact molecular mass to those in the amino acid standard run on the same day: 1. D-aspartic acid; 2. L-aspartic acid; 3. L-glutamic acid; 4. D-glutamic acid; 5. D-serine; 6. L-serine; 7. glycine; 8. β-alanine; 9. D-alanine; 10. γ-ABA; 11. L-alanine; 12. D-β-ABA; 13. α+β-AIB; 14. L-β-ABA; 15. L-valine; 16. ε-amino-*n*-caproic acid (EACA).

5.3.3.1 Shisr 033 amino acid composition and comparison to other carbonaceous chondrites

The typical HPLC-FD chromatograms of the acid hydrolysed hot-water extracts of the Shisr 033, Orgueil and Murchison meteorites, and a serpentine blank, are shown in Fig. 5.3, and the corresponding amino acid abundances in Table 5.4. The Shisr 033 meteorite was compared to these two other carbonaceous chondrites because, Murchison is a well-studied sample (and therefore can be used as a reference to confirm accurate measurements), and Orgueil is a CI1 type, which allows the amino acid composition to be compared to that in the alleged CI inclusion present in Shisr 033 (Russell *et al.* 2004). We also compared Shisr 033 to literature data of the CR chondrite Renazzo (Botta *et al.* 2002). The most abundant amino acids in Murchison are D- and L-isovaline (with 2493 and 2297 ppb, respectively), followed by α-AIB (with 1923 ppb). Glycine, β-alanine and D- and L-alanine are also present (Table 5.4).

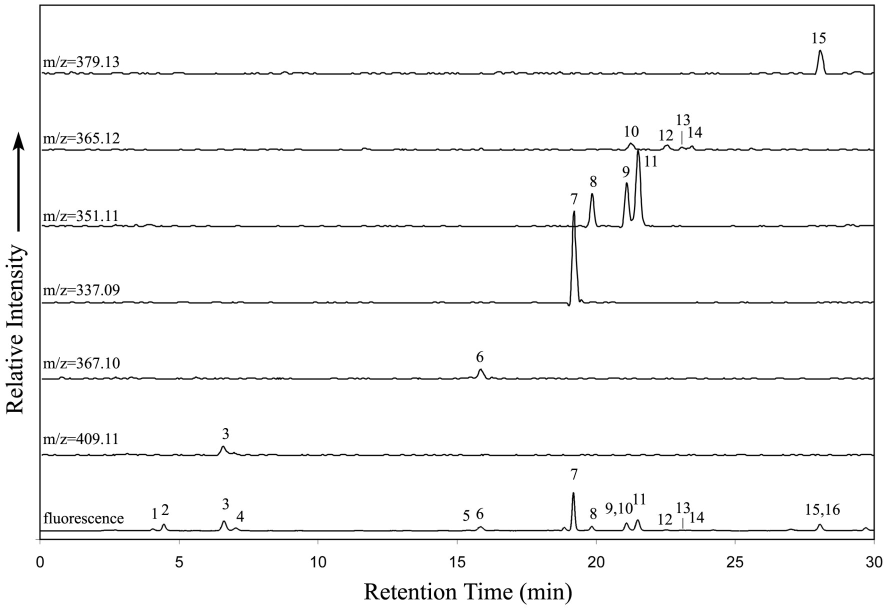

Fig. 5.5 - The 0 to 30 min region of the HPLC-FD and ToF-MS chromatograms of the Shisr 033 meteorite acid hydrolysed water extract. The peaks were identified by comparison of the retention time and exact molecular mass to those in the amino acid standard run on the same day: 1. D-aspartic acid; 2. L-aspartic acid; 3. L-glutamic acid; 4. D-glutamic acid; 5. D-serine; 6. L-serine; 7. glycine; 8. β-Alanine; 9. D-alanine; 10. γ-ABA; 11. L-alanine; 12. D-β-ABA; 13. α+β-AIB; 14. L-β-ABA; 15. L-valine; 16. EACA. Aspartic acid (peaks 1–2) could not be identified by exact mass due to poor ionization of this compound during the analysis.

In the case of Orgueil, the most abundant amino acids are β-alanine (2784 ppb) and glycine (1040 ppb), with very low levels of isovaline and α-AIB (Table 5.4). All these values agree with analyses performed previously by other authors (Ehrenfreund *et al.* 2001; Botta *et al.* 2002). The Renazzo amino acid content (Botta *et al.* 2002) includes γ-ABA (1092 ppb), glycine (875 ppb), L-glutamic acid (856 ppb) and D,L-β-amino-*n*-butyric acid (534 ppb). Comparison of the absolute amino acid content of the CM2 Murchison, the CI1 Orgueil, and the CR Renazzo shows a distinct absolute amino acid distribution for Shisr 033 meteorite. In fact, Shisr 033 has a lower total amino acid content (3800 ppb) than any of these other carbonaceous chondrites. We have compared the relative amino acid content (glycine = 1) of Shisr 033 to the relative amino acid content of other carbonaceous chondrites (Table 5.7, Fig. 5.6). If CI-type inclusions were present in the Shisr 033, as suggested in the initial description (Russell *et al.* 2004), a high relative abundance of β-alanine, similar to the CI Orgueil, can be expected (Table 5.7, Fig. 5.6). However, as illustrated in Fig. 5.6, the relative amino acid distribution of Shisr 033 is dissimilar to the distribution of the CM and CI meteorites analysed. Shisr 033 has relative β-alanine and α-AIB abundances (0.32 and 0.06, respectively) similar to

Table 5.5 - Summary of the average total amino acid abundances (serpentine blank corrected) in the 6 M HCl acid hydrolysed hot-water extracts of the CR type carbonaceous chondrite Shisr 033, L6 ordinary chondrites Shisr 031 and Shisr 035, and three soil samples collect on the Oman desert[a] as measured by LC-ToF-MS[b].

Amino Acid	CR chondrite	L chondrites		Soil samples		
	Shisr 033	Shisr 031	Shisr 035	78	82	89
D-Aspartic acid	57 ± 5	< 5	126 ± 38	68 ± 2	20 ± 1	< 10
L-Aspartic acid	189 ± 23	< 3	398 ± 100	232 ± 53	36 ± 1	17 ± 1
D-Glutamic acid	124 ± 7	6 ± 1	50 ± 11	61 ± 3	24 ± 2	14 ± 1
L-Glutamic acid	489 ± 34	16 ± 2	156 ± 38	271 ± 5	81 ± 1	38 ± 2
D-Serine	32 ± 11	< 4	< 4	18 ± 2	< 4	< 3
L-Serine	140 ± 34	< 4	< 4	69 ± 16	< 4	< 2
Glycine	417 ± 55	24 ± 11	41 ± 13	183 ± 36	4 ± 2	7 ± 1
β-Alanine	62 ± 10	9 ± 2	8 ± 2	9 ± 3	2 ± 1	3 ± 1
γ-ABA)	49 ± 23	< 2	< 2	< 2	< 2	< 2
D-Alanine	274 ± 14	< 2	28 ± 11	23 ± 7	5 ± 2	< 2
L-Alanine	330 ± 59	< 3	49 ± 12	51 ± 11	17 ± 1	2 ± 2
D-β-ABA	< 6	< 2	< 2	< 2	< 3	< 3
L-β-ABA	< 4	< 2	< 2	< 2	< 3	< 3
α+β-AIB[†]	23	< 4	< 4	< 4	< 5	< 6
D,L-α-ABA[†]	< 5	< 2	< 2	< 2	< 2	< 2
D-Isovaline	< 3	< 3	< 3	< 2	< 2	< 2
L-Isovaline	< 5	< 6	< 6	< 3	< 4	< 4
EACA	< 3	< 4	< 4	< 4	< 5	< 5
D-Valine	8 ± 3	< 2	< 2	< 2	< 3	< 3
L-Valine	174 ± 19	2 ± 1	11 ± 3	53 ± 16	13 ± 2	7 ± 2
Total	**2300**	**60**	**870**	**1040**	**200**	**90**

[a]See Fig. 5.1 for exact location of sample collection.
[b]All values are reported in parts-per-billion (ppb) on a bulk sample basis. The associated errors are based on the standard deviation of the average value between two and four separate measurements (N) with a standard error, $\delta x = \sigma_x \cdot N^{-1/2}$.
[†]Enantiomers could not be separated under the chromatographic conditions.

Table 5.6 - Amino acid enantiomeric ratios in the CR carbonaceous chondrite Shisr 033 and in the soil sample 78 collect on the Oman desert.

Amino Acid	Enantiomeric Ratio (D/L)*		
	Shisr 033[a]	Shisr 033[b]	Soil 78 [b]
Aspartic acid	0.27 ± 0.03	0.30 ± 0.05	0.29 ± 0.07
Glutamic acid	0.24 ± 0.03	0.25 ± 0.02	0.22 ± 0.01
Alanine	0.39 ± 0.03	0.83 ± 0.15	0.45 ± 0.17
Valine	0.10 ± 0.08	0.05 ± 0.02	< 0.04

*The uncertainties are based on the absolute errors shown respectively in Table 5.4 and Table 5.5, and are obtained by standard propagation calculation.
[a]D/L ratios calculated from the concentrations reported in Table 5.4, measured by HPLC-FD.
[b]D/L ratios calculated from the concentrations reported in Table 5.5, measured by LC-ToF-MS. Soil selected due to the higher total amino acid abundance.

Table 5.7 - Relative amino acid abundances (glycine=1) of several carbonaceous chondrites[a].

AA/Glycine	CM2	CM1	CR	CR[b]
	Murchison	**Orgueil**	**Shisr 033**	**Renazzo**
β-Alanine	0.71	2.68	0.32	0.25
D-Alanine	0.43	0.21	0.53	< 0.04
α-AIB	1.35	0.07	0.06	< 0.08
γ–ABA	0.45	0.39	0.08	1.25

[a]Relative amino acid abundances calculated from the absolute amino acid concentrations reported in Table 5.4, measured in this study by HPLC-FD, for the CM2 Murchison, the CI1 Orgueil, and the CR Shisr 033 meteorites.
[b]The data for the Renazzo meteorite was calculated from previous analyses (Botta *et al.* 2002). In case only upper limits of the absolute concentrations were measured, upper limits for the relative concentrations were calculated.

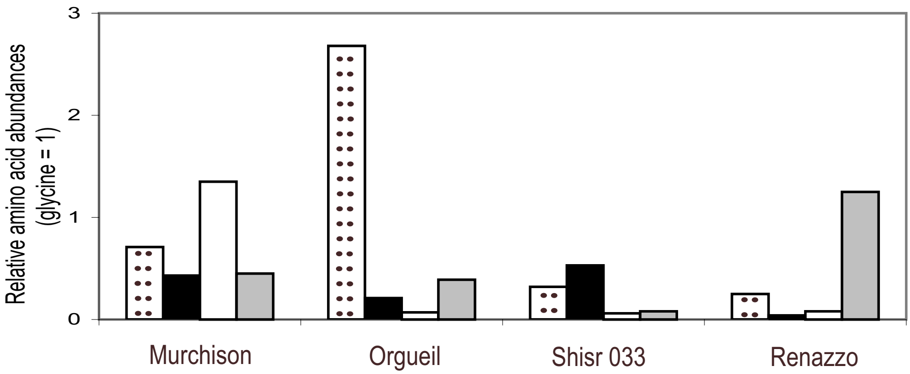

Fig. 5.6 - A comparison of the relative amino acid abundances (glycine = 1) of β-alanine (dots), D-alanine (black), α-AIB (white), and γ-ABA (grey) in the acid-hydrolysed hot-water extract of different carbonaceous chondrites. The relative amino acid abundances were calculated from the absolute amino acid concentrations reported in Table 5.4, measured in this study by HPLC-FD, for the CM2 Murchison, the CI1 Orgueil, and the CR Shisr 033 meteorites. The data for the Renazzo meteorite was calculated from previous analyses (Botta *et al.* 2002). In the case of D-alanine and α-AIB present in the Renazzo meteorite, only upper limits of the absolute concentrations were measured and therefore only upper limits for the relative concentrations were calculated.

the ones in the CR chondrite Renazzo (0.25 and <0.08, respectively), but all other relative amino acid abundances are significantly different (Table 5.7). Our data suggests that the fraction of fines of Shisr 033 analysed in our study does not correspond neither to a typical CI type nor to the CR Renazzo, which is the only CR analyzed for amino acids so far.

5.3.4 Oxygen and carbon isotopes

The oxygen isotopic composition of the whole-rock and components in Shisr 033 are shown in Table 5.8 and plotted in Fig. 5.7. The whole rock samples (WR and washed WR) and the chondrule composite all have oxygen isotopic signatures indistinguishable from other CR2 meteorites. The oxygen isotopic composition of whole rock samples of CR2s fall along a mixing line of slope 0.7, with anhydrous silicates primarily at the ^{16}O-rich end and hydrous matrix and dark inclusions at the ^{16}O-poor end of the mixing line (Weisberg *et al.* 1993). The unwashed whole rock sample (WR) plots approximately mid-way along the mixing line suggesting that the oxygen isotopic composition is a mixture of anhydrous and phyllosilicate material from either end of the mixing line. However, it is not clear what is the influence of terrestrial weathering (grade W2), in the form of metal oxidation and iron hydroxide staining. The sample washed in ethanolamine thioglycollate, which largely removed the iron-hydroxides, has an oxygen isotopic composition at the ^{16}O-rich end of the CR2 mixing line, where CR2s are dominated by anhydrous phase, such as LEW 85332, a meteorite that shows no evidence of aqueous alteration (Clayton and Mayeda 1999).

The efficiency and effects of the ethanolamine thioglycollate wash on the samples, in terms of oxygen isotopic measurements, has been assessed using a suite of variable weathered H chondrites collected in the Tenere region of Niger (Schultz *et al.* 1998), which is a hot desert area on similar latitude to that of Oman. Unwashed samples collected from the Tiffa and Grein areas fall along a common mixing line between typical H chondrite values and a point on the terrestrial fractionation line with $\delta^{18}O \approx 8‰$ (Fig. 5.8). The oxygen isotopic composition of the ethanolamine thioglycollate washed samples, in the case of the lightly weathered Grein 003 is now indistinguishable from typical H chondrite falls, while the heavily weathered Tiffa 001 is now much closer to that of the H chondrite falls, although it would appear that some weathering persists. The equilibrated H chondrites used in this study contain only well crystallised ferro-magnesian silicates and some feldspathic phases, but results show that the ethanolamine thioglycollate wash method is extremely efficient at removing alteration phases from anhydrous silicates without noticeably affecting the bulk properties in terms of oxygen isotopic signature. Shisr 033 contains abundant (see section 5.3.1.) indigenous phyllosilicate-rich material, and therefore it is unlikely that the pre-atmospheric entry whole rock oxygen isotopic composition would plot at the anhydrous end of the CR2 mixing line. In addition, it is likely that the ethanolamine thioglycollate washing did not discriminate between asteroidal and terrestrial alteration products. That said it is interesting to note that the hot desert weathering in the Tenere samples has $\delta^{18}O$ of $\approx 8‰$, although it should also be noted that the $\delta^{18}O$ of the weathering products does appear to vary as indicated by the distinct isotopic composition of the heavily weathered

Table 5.8 - Oxygen isotopic composition of the Shisr 033 meteorite (whole rock, chondrules and dark clast) measured by laser fluorination.

Sample	Sample Type	$\delta^{17}O$ (‰)	$\delta^{18}O$ (‰)	$\Delta^{17}O$
B	Whole rock	-0.59	2.29	-1.78
B	Whole rock	-0.70	2.21	-1.85
B2	Washed whole rock*	-2.33	0.14	-2.40
H	Chondrules	-1.55	1.20	-2.17
H	Chondrules	-1.45	1.41	-2.18
D	Dark clast	-4.59	-1.22	-3.96

*Treated with ethanolamine thioglycollate

H5-6 from Adrar Madet (Fig. 5.8). Assuming a $\delta^{18}O$ value of ≈ 8‰ for the Oman weathering products, then any mixing line between CR2 and terrestrial weathering would be unresolvable from the indigenous CR2 mixing line. It is not unreasonable to assume a $\delta^{18}O$ ≈ 8‰ value, given Oman local rain water has $\delta^{18}O$ values between –4.3 and +1.4‰ VSMOW (Waber 2006), based on rainwater samples collected near Haima during the meteorite search project in 2005. Additionally, $\delta^{18}O$ values of monsoon precipitation given by Fleitmann *et al.* (2004) range between -0.3 and 1.0‰ (VSMOW).

The oxygen isotopic composition of the phyllosilicate-rich, dark inclusion (sensu Weisberg *et al.* 1993; sample D) is not consistent with typical CR2 matrix or dark inclusions found in CR2s (Fig. 5.7), but instead falls in the range of typical CV3 or CK carbonaceous chondrites (Clayton and Mayeda 1999), and close to those of CO3s (Greenwood and Franchi 2004).

The nature of the carbon present in the phyllosilicate-rich dark inclusion D was investigated by stepped combustion, the results shown in Table 5.9 and Fig. 5.9. The carbon inventory is dominated by a large release (2.3 wt% C), in the range 550-650^{o}C, typical of carbonates (Wright and Pillinger 1989). The $\delta^{13}C$ of this component is around -8‰, much less than typical values ($\delta^{13}C$ of 30 to 65‰) for carbonates in carbonaceous chondrites (Grady *et al.* 1988), and more typical of terrestrial carbonate deposits ($\delta^{13}C$ of -5.31 to -9.07‰) as found in the desert regions of Oman where Shisr 033 was collected (unpublished data, University of Bern). At lower temperatures (150-350˚C) there is evidence of a smaller release of organic carbon (0.4 wt% C), with $\delta^{13}C$ values ranging from -34 to -19‰. The majority of this carbon appears to be terrestrial contamination, which typically has a $\delta^{13}C$ value of -35 to -25‰, and is quite distinct from indigenous organic carbon found in carbonaceous chondrites with $\delta^{13}C$ values of -18 to -10‰ (e.g. Botta and Bada 2002). It may be that the small amount of carbon above 300˚C is largely indigenous as the isotopic composition approaches that expected from meteoritic macromolecule, however, this component is only present at the level of no more than 0.2 wt% C, assuming some overlap with the carbonate peak.

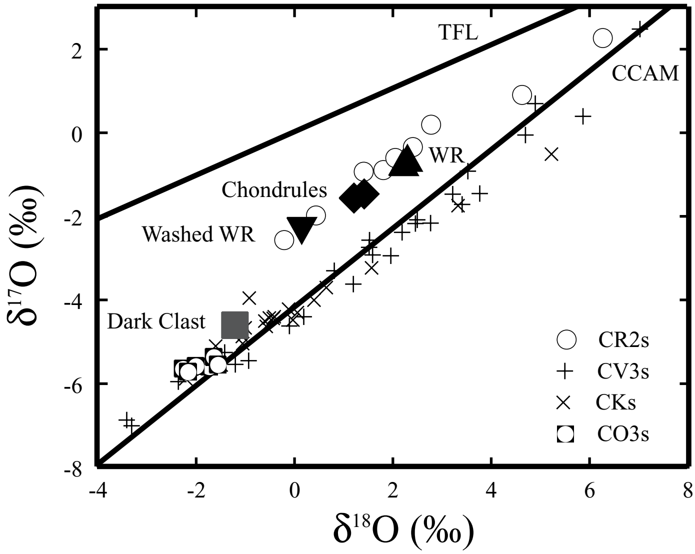

Fig. 5.7 - Oxygen isotopic composition of Shisr 033 and other carbonaceous chondrite groups. Filled symbols for Shisr 033: whole rock sample (WR ▲); composite of chondrules (chondrules ♦); whole rock sample washed in ethanolamine thioglycollate (washed WR ▼); hand picked phyllosilicate rich dark clast inclusion (dark clast ■). The terrestrial fractionation line (TFL) and carbonaceous chondrite anhydrous mineral (CCAM) line are shown for reference. CR2, CV3 and CK data from Clayton and Mayeda (1999), CO3 data from Greenwood and Franchi (2004).

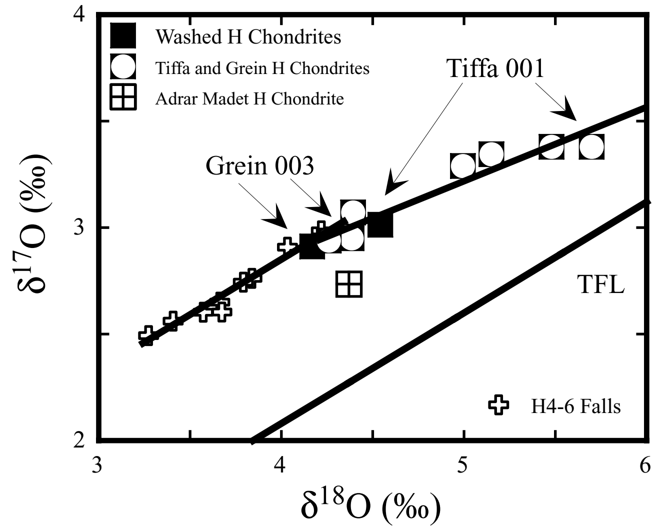

Fig. 5.8 - Oxygen isotopic composition of weathered and washed H chondrites from Tenere, Niger. It illustrates the efficiency of the ethanolamine thioglycollate wash method at removing terrestrial weathering products from anhydrous silicates, without affecting the indigenous oxygen isotopic composition.

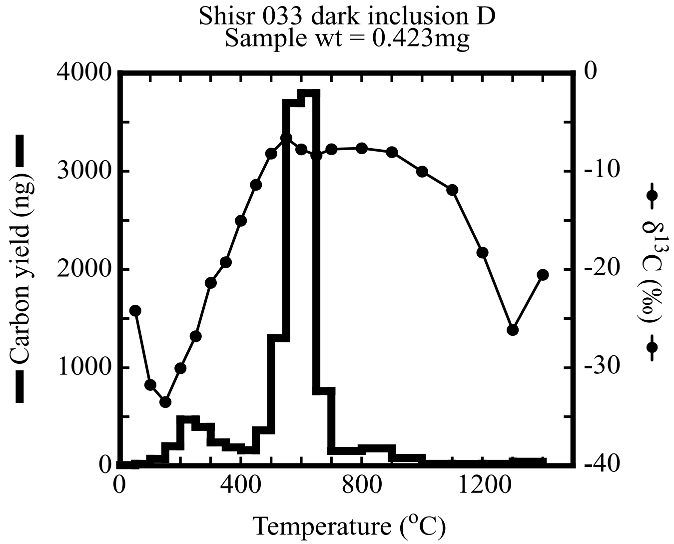

Fig. 5.9 - Stepped combustion profile of a dark inclusion (D), showing yield (bold histogram plot) and isotopic composition (point/line plot) with increasing temperature. Organics are oxidised between 200 and 500°C, while carbonates generally decompose between 500 and 700°C.

Table 5.9 - Stepped combustion data from a phyllosilicate-rich dark inclusion D, which contains 2.88 wt% carbon.

Temperature (°C)	**C yield (ng)**	**δ^{13}C (‰)**
50	7.1	-24.2
100	21.1	-31.8
150	71.2	-33.5
200	199.2	-30.1
250	471.2	-26.8
300	398.0	-21.3
350	239.2	-19.3
400	188.0	-15.0
450	160.9	-11.4
500	360.6	-8.2
550	1300.1	-6.6
600	3693.9	-7.8
650	3796.0	-7.6
700	760.7	-7.8
800	150.5	-7.6
900	177.9	-8.0
1000	80.6	-10.0
1100	20.5	-11.9
1200	18.5	-18.3
1300	20.3	-26.1
1400	41.0	-20.5

Table 5.10 - Terrestrial age of the carbonaceous chondrite Shisr 033, the L6 ordinary chondrites Shisr 031 and Shisr 035 as measured by AMS.

	Meteorites				
	Shisr 031	Shisr 033 (A)	Shisr 033 (B)	Shisr 033 (C)	Shisr 035
Type	L6	CR (bulk slices)	CR (bulk ground)	CR (bulk ground)	L6
Weight (g)	0.390	0.269	0.081	0.113	0.154
Chemical treatment	Acid etch	Acid etch	Acid etch	Acid etch	Acid etch
Fm	0.5439	1.0189	0.8992	1.9680	0.0530
Error	0.0056	0.0095	0.0063	0.0180	0.0013
CO_2 (cc)	0.59	0.78	0.57	0.33	0.17
Diluted (cc)	0.59	0.78	0.57	0.33	2.117
^{14}C atoms	$7.994x10^6$	$2.164x10^7$	$1.352x10^7$	$1.746x10^7$	$1.982x10^6$
^{14}C/weight (g)	$2.050x10^7$	$8.046x10^7$	$1.668x10^8$	$1.542x10^8$	$1.284x10^7$
Bulk ^{14}C (dpm/kg)	4.72	18.52	38.38	35.49	2.95
Error (dpm/kg)	0.18	0.31	0.89	0.69	0.45
Saturated activity†	51.1	51.1	51.1	51.1	51.1
^{14}C age (kyr)	19.7	8.4	2.4	3.0	23.6
Error (kyr)	1.3	1.3	1.3	1.3	1.8
Bulk ^{10}Be (dpm/kg)	11.70	16.04			15.95
Error (dpm/kg)	0.23	0.34			0.28
$^{14}C/^{10}Be$	0.40	1.15			0.18
$^{14}C/^{10}Be$ age (kyr)	15.0	6.4			21.4
Error (kyr)	0.4	0.2			1.3

†When class is not known, ^{14}C saturated activity of L chondrites (51.1 dpm/kg) was used.

5.3.5 Terrestrial ages and their relationship to the extend of terrestrial contamination

The terrestrial age of the carbonaceous chondrite Shisr 033, as well as the terrestrial ages of the ordinary chondrites Shisr 031 and Shisr 035 are summarised in Table 5.10. The expected ^{14}C saturation value was approximated by using the value for L chondrites (51.1 dpm kg^{-1}) for subsamples A, B and C. For Shisr 033 a $^{14}C/^{10}Be$ terrestrial age of 6.4 ± 0.2 kyr was obtained, which is much younger than those of the two L6 chondrites Shisr 031 (15.0 ± 0.4 kyr) and Shisr 035 (21.4 ± 1.3kyrs). The relatively low terrestrial age of a few thousands years of Shisr 033 is consistent with the low degree of weathering (W2) of the iron metal in this meteorite. In that sense, the first thought would be that the older age of the other two ordinary chondrites would lead to a higher degree of terrestrial contamination of those samples, compared to Shisr 033. However, as our amino acid analysis shows, the Shisr 033 meteorite has a higher contamination degree than Shisr 031 and Shisr 035 (see section 5.3.3.). Three possibilities can be invoked to explain this. First of all, the fact that the meteorites landed in different locations (Fig. 5.1) exposed them to different local terrestrial environments (see section 5.3.3.). The second possibility is the difference in porosity between the CR Shisr 033 and in the ordinary chondrites, as carbonaceous chondrites have, on average, a higher porosity (ranging from 24% to 35%) than L6 chondrites (ranging from 0% to 10%) (Consolmagno and Britt 1998). Although Oman is a desert, there is occasional precipitation (Sanlaville 1992; Al-Kathiri *et al.* 2005), including monsoons, during which soil material can be percolated through the meteorites. A higher porosity, and therefore a higher internal surface, probably increases the changes for absorption of organic material from the soil. A third possibility is the difference in the oxidation state of iron present in the meteorites studied. The significantly higher abundance of metallic iron in Shisr 033 (see section 5.3.1. and 5.3.2.) may serve as a nutrient for iron-oxidising microorganisms that colonialise the meteorite, leading to higher amino acid contamination degree in the CR meteorite. This colonialisation is less likely in the L6 chondrites due to their higher content of oxidised iron.

5.4 Conclusion

We have performed for the first time a multidisciplinary analysis of the Shisr 033 meteorite, collected in the Oman desert. The initial classification as a CR chondrite is confirmed by bulk chemical analyses as well as oxygen isotopes, these latter showing that Shisr 033 falls into the CR2 group. Based on oxygen isotopes, dark inclusions hosting organic material are more closely related to CV3-CO3 chondrites than CR2 bulk material. Amino acid analysis shows no evidence for CI- or CM-like material in these inclusions.

Amino acid and carbon isotopic data indicate high terrestrial contamination in Shisr 033. Both the Shisr 033 meteorite and the Oman soil samples show that L-amino acids and glycine were the most abundant amino acids. Additionally, Shisr 033 D/L proteic amino acid ratios are generally smaller than 0.4 and in agreement with the D/L amino acid ratios of the Oman desert soils. Carbon isotope analysis of a Shisr 033 dark inclusion revealed high carbonate contents, with a $\delta^{13}C$ value of –8‰ (falling within the range of typical terrestrial carbonates of the Oman desert), and low organic carbon content with $\delta^{13}C$ values ranging from -34 to -19‰. However, the presence of a small fraction of indigenous extraterrestrial organic compounds in Shisr 033 cannot be excluded because the extraterrestrial amino acid α-AIB was preserved in this meteorite over thousands of years. Shisr 033 was found to have a terrestrial age of 6.4 ± 0.2 kyr, which is consistent with its low weathering of the metal. Differences in the amino acid contamination content between Shisr 033 and two ordinary chondrites (Shisr 031 and Shisr 035) also collected in the Oman desert can be explained by differences in the composition of their fall sites, in the porosity of these meteorites, in the abundances of metallic iron or a combination of these effects. This study supports previous observations that meteorites collected in hot deserts suffer significant terrestrial alteration and contamination during their residence time.

Acknowledgements

The authors would like to thank Dr. Linda Welzenbach (Smithsonian National Museum of Natural History, Washington DC, USA) for providing us with a Murchison meteorite sample, the Musée National, Paris for the Orgueil meteorite sample used in this study, and Zan Peeters for graphic support. This research was supported by Fundação para a Ciência e a Tecnologia (scholarship SFRH/BD/10518/2002), NWO-VI 016023003, PPARC and the NASA Astrobiology Institute at the Goddard Center for Astrobiology. Field work in Oman was supported by Swiss National Science Foundation grant 200020-107681.

References

Al-Kathiri A., Hofmann B. A., Jull A. J. T. and Gnos E. 2005. *Meteorit. Planet. Sci.* 40, 1215-1239.

Anders E. and Grevesse N. 1989. *Geochim. Cosmochim. Acta* 53, 197-214.

Ash R. D. and Pillinger C. T. 1995. *Meteoritics* 30, 85-92.

Bischoff A. and Geiger T. 1995. *Meteoritics* 30, 113-122.

Bischoff A. *et al.* 1993. *Geochim. Cosmochim. Acta* 57, 1587-1603.

Bland P. A., Berry F. J., Smith T. B., Skinner S. J. and Pillinger C. T. 1996a. *Geochim. Cosmochim. Acta* 60, 2053-2059.

Bland P. A., Franchi I. A., Sexton A. S., Berry F. J. and Pillinger C. T. 1996b. *Meteorit. Planet. Sci.* 31, page A16.

Bland P. A., Berry F. J. and Pillinger C. T. 1998a. *Meteorit. Planet. Sci.* 33, 127–129.

Bland P. A., Sexton A. S., Jull A. J. T., Bevan A. W. R., Berry F. J., Thornley D. M., Astin T. R., Britt D. T. and Pillinger C. T. 1998b. *Geochim. Cosmochim. Acta* 62, 3169–3184.

Botta O. and Bada JL. 2002. *Surv. Geophys.* 23, 411-467.

Botta O., Glavin D. P., Kminek G. and Bada J. L. 2002. *Orig. Life Evol. Biosph.* 32, 143 – 163.

Clayton R. N. and Mayeda T. K. 1999. *Geochim. Cosmochim. Acta* 63, 2089-2104.

Consolmagno G. J. and Britt D. T. 1998. *Meteorit. Planet. Sci.* 33, 1231-1241.

Cornish L. and Doyle A. 1984. *Palaeontology* 27:421-424.

Ehrenfreund P., Glavin D. P., Botta O., Cooper G. and Bada J. L. 2001. *Proc. Natl. Acad. Sci. USA* 98, 2138–2141.

Fleitmann D., Burns S. J., Neff U., Mudelsee M., Mangini A. and Matter A. 2004. *Quat. Sci. Rev.* 23, 935–945.

Franchi I. A., Bland P. A., Jull A. J. T., Cloudt S., Berry F. J. and Pillinger C. T. 1996. *Meteorit. Planet. Sci.* 31, A46-A47.

Gillet P., Barrat J. A., Beck P., Marty B., Greenwood R. C., Franchi I. A., Bohn M. and Cotten J. 2005. *Meteorit. Planet. Sci.* 40, 1175-1184.

Glavin D. P., Dworkin J. P., Aubrey A., Botta O., Doty III J. H., Martins Z. and Bada J. L. 2006. *Meteorit. Planet. Sci.* 41, 889–902.

Grady M. M., Wright I. P., Swart P. K. and Pillinger C. T. 1988. *Geochim. Cosmochim. Acta* 52, 2855-2866.

Greenwood R. C. and Franchi I. A. 2004. *Meteorit. Planet. Sci.* 39, 1823-1838.

Howe J. M., Featherston W. R., Stadelman W. J. and Banwartz G. J. 1965. *Appl. Microb.* 13, 650-652.

Jull A. J. T., Donahue D. L. and Linick T. W. 1989. *Geochim. Cosmochim. Acta* 53, 2095-2100.

Jull A. J. T., Wlotzka F., Palme H. and Donahue D. J. 1990. *Geochim. Cosmochim. Acta* 54, 2895-2898.

Jull A. J. T., Donahue D. J., Cielaszyk E. and Wlotzka F. W. 1993. *Meteoritics* 28, 188-195.

Jull A. J. T., Cloudt S. and Cielaszyk E. 1998. ^{14}C terrestrial ages of meteorites from Victoria Land, Antarctica and the infall rate of meteorites. In *Meteorites: Flux with time and impact effects.* Edited by McCall G. J., Hutchison R., Grady M.

M. and Rothery D. Geological Society of London Special Publication. pp. 75-91.
Kallemeyn G. W. and Wasson J. T. 1982. *Geochim. Cosmochim. Acta* 46, 2217-2228.
Lee M. R. and Bland P. A. 2004. *Geochim. Cosmochim. Acta* 68, 893–916.
Miller M. F., Franchi I. A., Sexton A. S. and Pillinger C. T. 1999. *Rapid Commun. Mass Spectrom.* 13, 1211-1217.
Pouchou J. L. and Pichoir F. 1984. *Rech. Aérospat.* 3, 167-192.
Ramseyer K., Fischer J., Matter A., Eberhardt P. and Geiss J. 1989. *J. Sediment. Petrol.* 59, 619-622.
Russell S. S., Folco L., Grady M. M., Zolensky M. E., Jones R., Righter K., Zipfel J., and Grossman J. N. 2004. *Meteorit. Planet. Sci.* 39, A215–A272.
Sanlaville P. 1992. *Paléorient* 181, 5-26.
Schultz L. *et al.* 1998. *Meteorit. Planet. Sci.* 33, A138-A138.
Slater-Reynolds V. and McSween H. Y. Jr. 2005. *Meteorit. Planet. Sci.* 40, 745-754.
Steele I. M. 1990. ACS Symp. 415, 150-164.
Stelzner TH. and Heide K. 1996. *Meteorit. Planet. Sci.* 31, 249-254.
Stelzner TH. *et al.* 1999. *Meteorit. Planet. Sci.* 34, 787-794.
Waber H. N. 2006. Institute of Geological Sciences, University of Bern, RWI Technical Report TR 06-04.
Weisberg M. K., Prinz M., Clayton R. N. and Mayeda T. K. 1993. *Geochim. Cosmochim. Acta* 57, 1567-1586.
Wright I. P. and Pillinger C. T. 1989. *U.S. Geological Surv.* 1890, 9-34.
Zhao M. and Bada J. L. 1995. *J. Chrom. A* 690, 55-63.